A CAVITATION RESISTANT HYDROSTATIC SEAL FOR HIGH PRESSURE BREAKDOWN

by

Warren C. Prouty

Senior Project Engineer

Sundstrand Fluid Handling Corporation

Arvada, Colorado

Derek S. Da Silva

Maintenance Engineer

Agrium Redwater Nitrogen Operations

Redwater, Alberta, Canada

and

Harry Farrell

Maintenance Technician

Agrium Carseland Nitrogen Operations

Carseland, Alberta, Canada

Warren C. Prouty is a Senior Project Engineer with Sundstrand Fluid Handling Corporation, in Arvada, Colorado. During his nine years at Sundstrand, he has held positions in Product Development and in the integral gear, multistage pump product group. He is coinventor of the hydrostatic seal technology covered in U.S. Patent No. 5,755,817, "Hydrostatic Seal," issued in May of 1998.

Mr. Prouty earned a B.S. degree (Mechanical Engineering) from the University of Colorado at Denver (1990). He is a registered Professional Engineer in the State of Colorado.

Derek S. Da Silva is a Maintenance Engineer at Agrium Redwater Nitrogen Operations, in Redwater, Alberta, Canada. He has been at Agrium for six years. He is currently involved in machinery monitoring, troubleshooting, and improvement projects. He earned a B.S. degree (Mechanical Engineering) from the University of Manitoba (1993). He is a registered Professional Engineer in the Province of Alberta.

Harry Farrell is a Maintenance Technician at Agrium Carseland Nitrogen Operations, Carseland, Alberta, Canada. During his 20 years at Agrium, he has been responsible for maintenance and troubleshooting of various plant equipment. He started his apprenticeship at Rolls Royce Aero Engine Division, where he worked for 20 years. He has extensive experience with Sundstrand integral gear, multistage pumps.

ABSTRACT

A unique hydrostatic throttle bushing concept has been developed and successfully tested. The throttle bushing is based on the concept of typical hydrostatic face seals, but incorporates improvements to minimize cavitation and maximize performance. Face geometry modifications include flow oriented feed slots to the hydropads and vortex pockets for minimizing cavitation damage. Parallelism between the throttle bushing and the mating ring is maintained with a face control groove, oriented to eliminate face distortion under high differential pressure loading. Additionally, materials selection has played a key role in the successful field operation of the hydrostatic throttle bushing. Currently there are three field installations in two stage, high energy, centrifugal pumps operating in urea production for ammonia feed. Operating successfully since 1997, the hydrostatic throttle bushing has proven to be a reliable, simple means of reducing stuffing box pressure in these applications.

INTRODUCTION

Hydrostatic face seals having a controlled leakage gap may be utilized for reliable service in low lubricity fluids when a controlled, but significant amount of leakage is acceptable. The controlled axial gap is determined by geometry features on the face, which develop a specific pressure profile. Slot fed hydrostatic seals are prone to cavitation damage when pressure drops across the face such that fluid velocities in the slot are high. This cavitation damage propagates from the slot across the face of the seal eliminating the hydrostatic features, and thereby causing face contact. A unique hydrostatic throttle bushing concept, described herein, incorporates geometry features on the face and a cavitation resistant material that allows successful application as a pressure breakdown device for high pressure drop conditions. Predicted results using a mathematical model, described herein, correlate well with lab test results for both water and ammonia.

The new hydrostatic throttle bushing has been applied to a two stage, high energy ammonia pump where the stuffing box pressure exceeds the capability of standard mechanical face seals. By dropping the pressure across the hydrostatic throttle bushing, lower stuffing box pressures can be achieved. Lower stuffing box pressure means a conventional dual seal arrangement can be used, which ensures an effective atmospheric seal, as well as simplifying the seal support system required for the pump.

HYDROSTATIC SEALS

Typically, hydrostatic seals have been applied in applications involving high surface velocities, high pressure drops, or where poor lubricity fluids have necessitated noncontacting faces. Some nuclear reactor coolant pumps (Lebeck, 1991), which require long life reliable seals, utilize hydrostatic seals due to their ability to operate in a noncontacting state under high pressures. In high pressure turbopumps for advanced storable liquid rocket engines, hydrostatic seals operate at 4000 psid at surface velocities of 600 ft/sec (Mallaire, et al., 1969). Hydrostatic seals operate at a fixed gap based on an opening force caused by the pressure distribution in the thin film separating the rotating and stationary elements. This opening force is balanced at a particular film thickness, by a closing force due to the sealed pressure and/or spring force. The pressure distribution is developed using externally pressurized recesses, or hydropads, in one face of the seal. These recesses are pressurized either by sealed pressure or by an external source through a series of orifices. These orifices can be capillaries, shown in Figure 1, that feed through from the pressure source or slots on the face that feed into the hydropads, as shown in Figure 2.

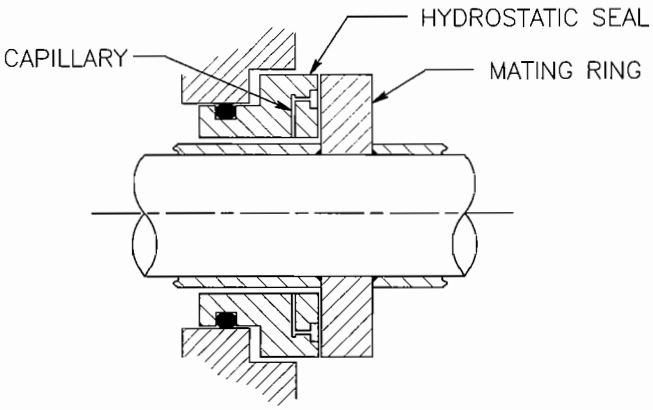

Figure 1. Capillary Controlled Hydrostatic Seal.

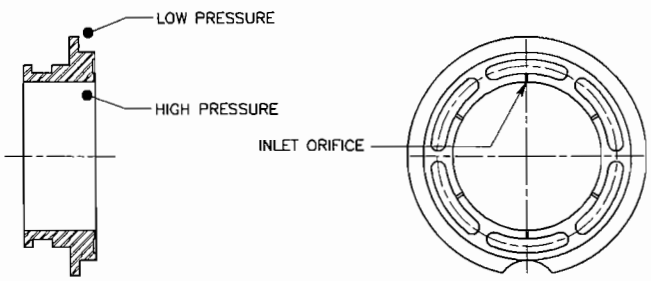

Figure 2. Typical Slot Fed Hydrostatic Seal Geometry.

The orifice sizing, and thus the pressure in the hydropad of the seal, determines the pressure profile and therefore the operating gap of the seal. Laurenson and O'Donoghue (1978) show the effect of varying the gap at the face of the hydrostatic seal. With reference to Figure 3, at a high value of gap, the flow across the face, which is a third order function of the gap, is large compared with the flow through the capillary (or slot). As a result, the pressure distribution approaches that of a typical face seal. At a low value of gap, the flow through the capillary (or slot) is large compared with the flow across the face. In this case, the hydropad pressure approaches the sealed pressure. Integrating the pressure distribution over the face area provides the opening force.

In order to minimize leakage while maintaining a pressure gradient across the face and "trackability" with axial perturbations

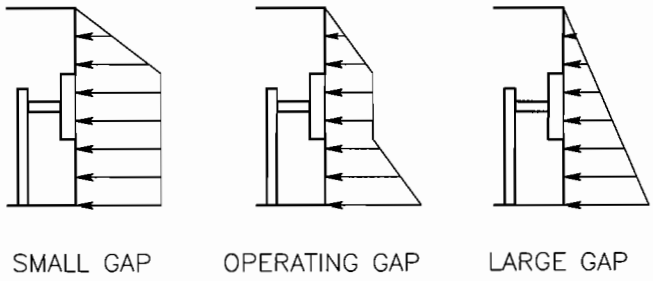

Figure 3. Face Pressure Profile as a Function of Face Gap.

(Laurenson and O'Donoghue, 1978), the stiffness and damping must be maximized at the face. Maximum damping is achieved by maximizing the area of close contact, whereas the stiffness is a function of the pressure profile. The closest area of contact lies in the inner and outer land that surround the hydropad.

Laurenson, et al. (1973), recommend a land width ratio (LWR) greater than .25 and less than .33, in order to maximize stiffness for a given leakage. The land width ratio is defined in Equation (1) (Figure 4).

$$LWR = C / (Ri - Ro) \quad (1)$$

Where:
LWR = Land width ratio
C = Land width
Ro = Outer radius
Ri = Inner radius

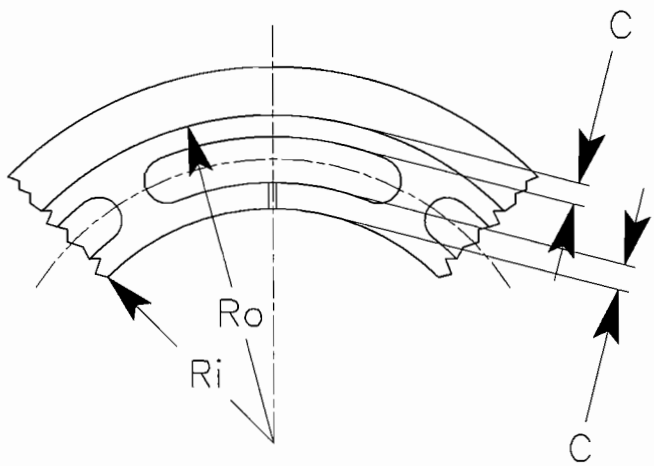

Figure 4. Hydrostatic Seal Geometry.

Two problems plague hydrostatic seals under high pressure drop conditions: excessive face deflections and cavitation damage. Like any seal under high pressure or high temperature conditions, the hydrostatic seal face can become concave or convex. This reduces the area of close contact and the hydrostatic effects of the seal. Ideally, the rotating and stationary elements of the seal should be parallel to each other.

Another effect of high differential pressure on the hydrostatic seal is high leakage rates that cause high fluid velocities in the slots. Because the fluids involved generally have low vapor pressures, the tendency is for cavitation inception to occur in the slot due to the high velocities. Cavitation erosion can propagate through the hydropad and across the outer land of the seal face. Cavitation erosion will eventually eliminate the hydrostatic features of the seal, thereby leading to face contact. A unique hydrostatic throttle bushing concept recently developed addresses these issues and is considered in detail in the following sections.

FIRST GENERATION HYDROSTATIC THROTTLE BUSHING

The original requirement for applying a hydrostatic seal as a pressure breakdown device was a two stage, high energy pump in ammonia service. The process seal on the second stage had an excessive pressure limit due to the head rise from the first stage. Previously, allowable operating stuffing box pressures were achieved on stage two through a series of dynamic rotors and stators that energized low pressure process fluid. The process diagram for a typical rotor installation is shown in Figure 5. Flush flow was introduced into the stuffing box of the second stage to keep the mechanical seal clean and cool. The flush fluid then flowed across the dynamic rotors and back to suction of stage two, where it entered the process stream.

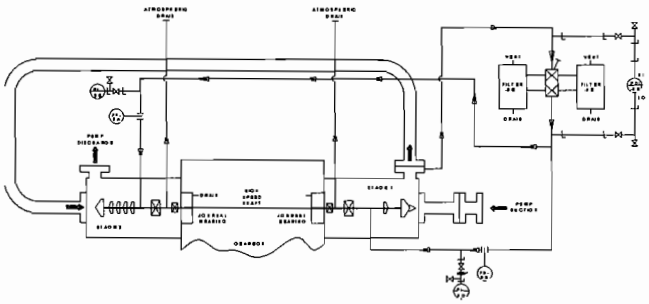

Figure 5. Typical Dynamic Rotor Process Diagram for Two Stage Pump.

The hydrostatic seal offered an improvement over the dynamic rotors and stators. The rotors and stators consisted of numerous parts, assembled in a specific order with a high potential for assembly errors. Axial clearances on the dynamic rotors are small, requiring close attention to assembly sequence and technique. Power consumption ranged from 5 hp to 20 hp.

The hydrostatic seal provided not only a simpler system, but a more robust and less costly method for achieving low stuffing box pressure as well. The pressure reduction of the original hydrostatic seal application was 1450 psid, resulting in a stuffing box pressure of 350 psig. This pressure drop was achieved at a flowrate of 4 gpm. Material selection for the original design was 4140 steel, due to its strength and commonality with other components of the pump. During water testing in the shop, the hydrostatic seal showed initial favorable results. However, performance degraded over short time periods once the seal was applied to ammonia process in the field. Two modes of failure were apparent that negated the hydrostatic effects of the seal: cavitation damage and excessive distortion of the face under pressure. Varying degrees of erosion damage to the faces of the hydrostatic seals were limiting life to less than three months. In one instance, a hydrostatic seal with only three weeks of operation had sufficient erosion damage to render the hydrostatic effects useless. Evidence showed that once the hydrostatic features were affected, the seal would operate as a contacting face seal and wear accordingly. In addition, finite element analysis showed excessive deflection of the hydrostatic seal under pressure, resulting in a convex face. Micromeasurements on the face showed 40 μ-in more wear at the inner land area, indicating rubbing contact. These measurements were consistent with the finite element analysis results shown in Figure 6.

Contact of the seal face, by either cavitation or deflection, generated heat that raised the process fluid temperature at the seal face, causing vaporization. This accelerated the cavitation effects. Damage extent on the faces ranged from slight erosion, as shown in Figure 7, to complete destruction of the hydrostatic pads. In one case, serpentine leakage paths were eroded into the solid face after the recesses were worn away, as shown in Figure 8.

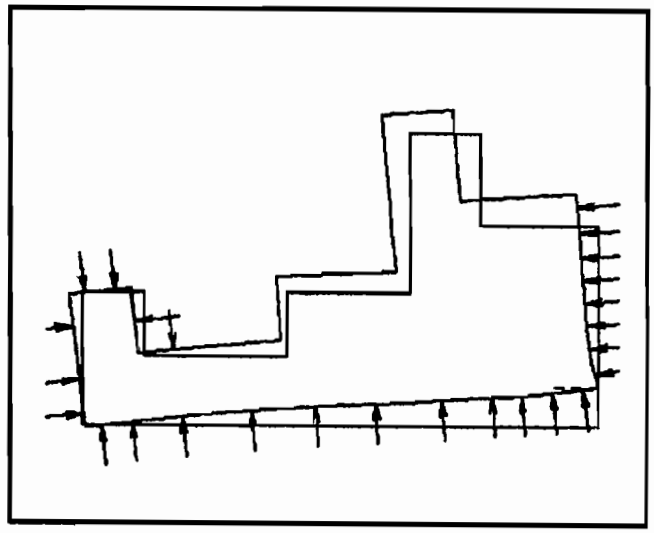

Figure 6. Finite Element Analysis Results, Hydrostatic Seal.

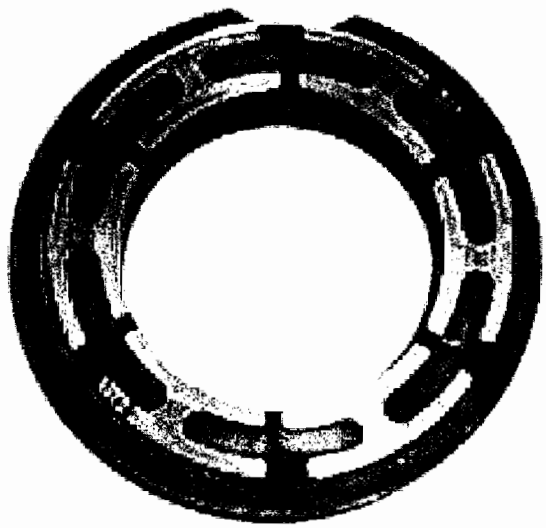

Figure 7. Worn Hydrostatic Seal.

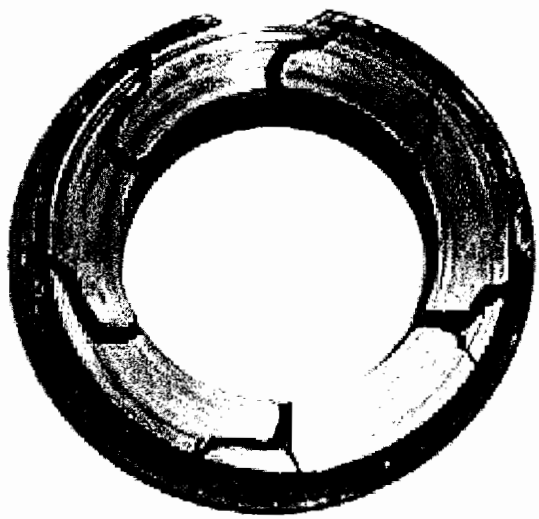

Figure 8. Worn Hydrostatic Seal.

The eroded zones showed damage more common to cavitation than to high velocity abrasion, as would be seen with fluid borne particulate. The orifice entrances to each hydropad were eroded on the pressure side of the channel, where the flow must make a 90 degree turn from a rotational to radial path. It was concluded that the deviation of streamlines from their circumferential trajectory to a radial trajectory into the orifice slot was resulting in cavitation inception at the orifice entrance. This damage was further enhanced by excessive deflection of the face, which caused contact at the inner land.

The fact that the water test results had proven favorable, even under the same pressure loading, could be explained by the viscosity of cold water. It had almost double the viscosity of ammonia, and thus produced a sufficiently large film at the seal face to mask face deflection under pressure and thus avoid contact. These initially poor field results forced removal of the hydrostatic seal and reinstallation of the seal rotor system.

SECOND GENERATION HYDROSTATIC THROTTLE BUSHING

A redesign effort focused on two major design flaws seen in the original design: deflection of the seal face and propensity for cavitation. Research of the literature provided clues to the field test failure. Metcalfe (1972) identified five main factors to prevent contact in practical application of hydrostatic seals:

- Orifices used to throttle flow to pockets in the seal face must not become restricted or blocked.
- Distortions due to pressure and temperature effects must not be significant compared with nominal separation.
- Sufficient pressure differential must be maintained across the seal.
- Erosion and wear of seal faces must be negligible.
- Resistance of the seal to axial and tilting disturbances must be sufficiently high.

The objectives of the redesign effort were to satisfy all the design criteria noted above. It was determined that several design changes to the geometry of the throttle bushing were necessary. In addition, a stiffer material would help eliminate the deflection problems seen during the initial field tests of the hydrostatic throttle bushing. Changes to the geometry of the seal and material changes were finalized, utilizing finite element analysis and mathematical modelling to aid in developing a functional design. Hydrostatic feature proportions were modified based on Laurenson, et al. (1973), in order to optimize leakage, film stiffness, and stability. These include inner and outer land widths, hydropad width and depth, and number of hydropads. Improved geometry features are shown in Figure 9. They include a face control groove to help balance the face under pressure loading and maintain parallelism to the mating ring, geometry changes to the hydrostatic features for cavitation prevention, and utilization of a hard, cavitation resistant material more able to withstand cavitation damage.

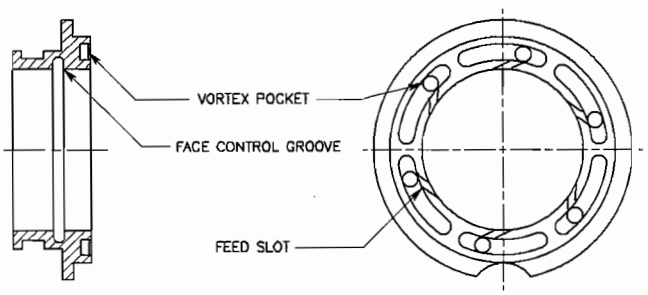

Figure 9. Hydrostatic Throttle Bushing Geometry Improvements.

CAVITATION RESISTANT GEOMETRY

The main design requirement of the improved hydrostatic seal was to eliminate or accommodate the cavitation that was so prevalent in the first generation hydrostatic seal. One unique part of the design was to develop improvements that eliminated the convoluted fluid path in order to prevent the inception of cavitation. By orienting the feed slots tangential to the flow, the path of the fluid is less torturous. Making a smooth, tangential transition eliminates the sudden pressure drop associated with the turn from circumferential to radial flow. The edges at the entrance of each orifice feed slot were radiused to enhance this feature. Further, in order to make a more robust design, a method of capturing vapor bubbles that may form in the orifice feed slots was included. Using the theory of inertia separation, vortex pockets were added to the bottom of each hydropad at the orifice inlet. The orifice inlet is oriented tangential to the vortex pocket inducing a swirling flow. The swirling flow causes a vortex. The vortex drives the dense fluid outward to the walls of the pocket and out into the hydropad, while the low pressure region inside the vortex contains less dense vapor bubbles. The vapor bubbles are thereby prevented from collapsing on a surface critical to the performance of the seal.

MATERIALS

Because of the deflections encountered on the first generation hydrostatic throttle bushing, it was determined that the new material of choice would need to be stiffer and more resistant to cavitation. Coincidental to the redesign effort on the hydrostatic throttle bushing, independent materials testing was being carried out to find a more cavitation resistant material than the typical stainless steel alloys previously applied to pump components. Materials testing had shown particularly positive results with a material called Ultimet® alloy. It had markedly superior cavitation resistance to any of the other materials tested. Additionally, results of ASTM G-76 (Modified) tests, carried out by the manufacturer, showed equally impressive results as shown in Table 1 (Haynes, 1994).

Table 1. Cavitation Erosion Data.

Wrought Alloys	Cavitation Erosion Depth in mm
Ultimet® Alloy	.0068
Hastelloy C-276 Alloy	.1128
Type 316L Stainless Steel	.1802
Type 410 Stainless Steel	.2151
Hastelloy C-22 Alloy	.1122
Hastelloy G-30 Alloy	.1225
Ferralium 255 Alloy	.1336
Nitronic 60 Alloy	.0173
Sandvik 2205 Alloy	.1481
Stellite 6 Alloy (Weld)	.0099

This cobalt based alloy exhibits high cavitation resistance in addition to being of high stiffness and strength. Hardness of the alloy is almost two times that of 4140 steel and the modulus of it is 33.2×10^6 lb/in^2 versus 30×10^6 lb/in^2 for 4140 steel. The alloy is cobalt based with chromium, molybdenum, and tungsten for corrosion resistance. As a result of these findings, the previously tested alloy was selected for the hydrostatic throttle bushing.

FACE CONTROL GROOVE

According to Metcalfe (1972), distortions due to pressure and temperature effects must not be significant compared with nominal separation. Even with the use of hard stiff materials, deflections at the face of the hydrostatic throttle bushing under pressure, while improved, still proved excessive according to finite element

analysis. Therefore, some other means were necessary to achieve the flat face under high pressure and potentially high temperature conditions. Through utilization of finite element analysis, a face control groove was added to the geometry of the hydrostatic throttle bushing that sufficiently reduced face deflections below expected nominal separation, as shown in Figure 10.

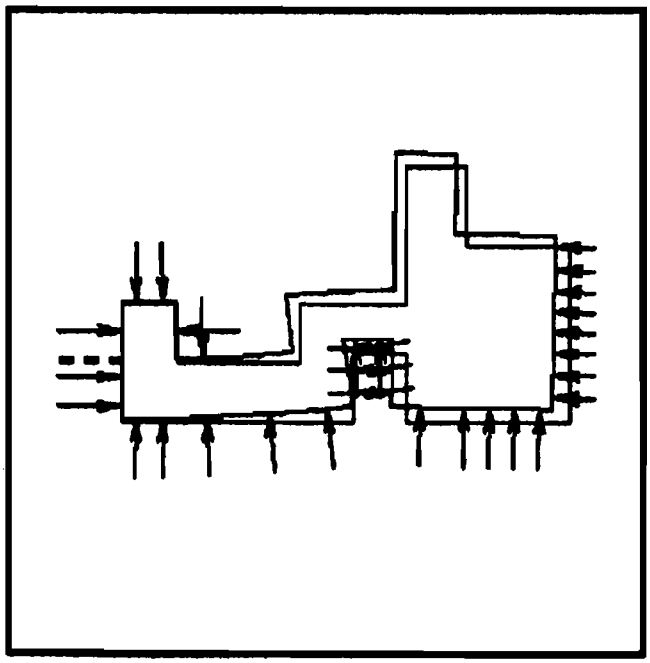

Figure 10. Finite Element Analysis Results with Face Control Groove.

The face control groove allows the body of the throttle bushing to rotate with pressure and temperature while maintaining flatness at the face. Decoupling of the face is accomplished by a localized thin section that permits easy relative deflection. Sizing and location of the groove is based on a range of pressures and temperatures and can be changed for specific applications through finite element analysis. This groove can be located on either the outer diameter or the inner diameter of the throttle bushing, depending upon the application (Prouty and Bond, 1998). Test hardware was manufactured with the groove on the inner diameter in order to allow for an O-ring sealing surface at the outer diameter of the throttle bushing.

MODELLING

In order to apply the hydrostatic seal to a variety of process fluids under a variety of operating conditions, a sizing model was developed using MathCAD® software. The model, based on calculations in Laurenson and O'Donoghue (1978), calculates the operating gap and the leakage of the hydrostatic throttle bushing given geometry, process fluid properties, and overall pressure differential. By having geometry as an input, the user has the ability to vary the stiffness and damping, based on location and width of inner and outer lands and hydropad configuration.

Closing forces at the face, based on sealed pressure and throttle bushing geometry, are calculated using Equation (2).

$$Fclose = \pi \times Pe \times (R4^2 - R5^2) + \pi \times Ps \times (R5^2 - R1^2) \quad (2)$$

Laurenson and O'Donoghue (1978) calculate the thrust force on the seal face using Equation (3).

$$Fthrust=\pi\times(Pt-Pe)\times\left[\frac{(R4^2-R3^2)}{2\times\ln\left(\frac{R4}{R3}\right)}-\frac{(R2^2-R1^2)}{2\times\ln\left(\frac{R2}{R1}\right)}\right]$$
$$+\pi\times(Ps-Pe)\times\left(\frac{R2^2-R1^2}{2\times\ln\left(\frac{R2}{R1}\right)}\right)-\pi\times Ps\times R1^2+\pi\times Pe\times R4^2 \quad (3)$$

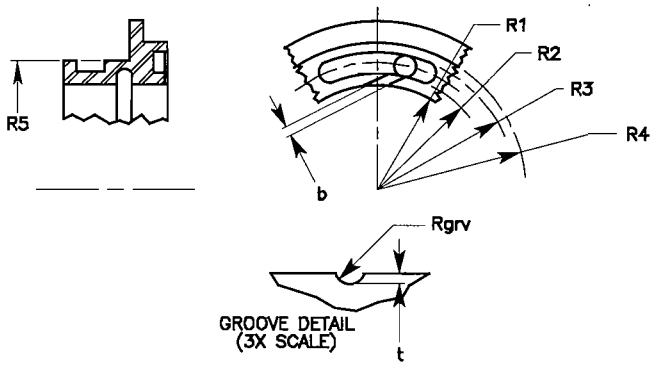

Figure 11. Hydrostatic Throttle Bushing Geometry.

Cheng, et al. (1968), gave the maximum achievable load generated by hydrodynamic action as Equation (4).

$$Fhydrodynamic = fd \times\left(\frac{6 \times \mu \times U \times b \times A}{h^2}\right) \quad (4)$$

Where:
fd = Geometry factor
μ = Fluid viscosity, lb-sec/in^2
U = Tangential velocity, in/sec
b = Width of sealing surface, in
A = Sealing surface area, in^2
h = Film thickness, in

Expanding Equation (4) and applying to the inner and outer lands yields Equation (5).

$$Fhydrodynamic=Yin\times\left[6\times\mu\times\varpi\times\pi\times\left(\frac{(R2^2-R1^2)^2}{hinner^2}\right)\right]$$
$$+Yout\times\left[6\times\mu\times\varpi\times\pi\times\left(\frac{(R4^2-R3^2)^2}{houter^2}\right)\right] \quad (5)$$

The force balance is one of three equations with three unknowns that are solved simultaneously. The three equations are:

- Using Equations (2), (3), and (5), the force balance equation is shown in Equation (6).

$$Fthrust + Fhydrodynamic - Fclose - Fspring = 0 \quad (6)$$

- The flow across the outer land is equal to the sum of the flow across the inner land and the flow through the orifice feed slots, which is represented by Equation (7).

$$Qouterland = Qorificefeedslot + Qinnerland \quad (7a)$$

Expanding, Equation (7a) becomes Equation (7b)

$$\pi\times\frac{houter^3}{12\times\mu}\times\left(\frac{R4+R3}{R4-R3}\right)\times(Pt-Pe)=\frac{Agrv}{\sqrt{\frac{\rho}{2}\over(Ps-Pt)\times386.4}}\qquad(7b)$$

$$+\pi\times\frac{hinner^3}{12\times\mu}\times\left(\frac{R2+R1}{R2-R1}\right)\times(Ps-Pt)$$

- The relation between the gaps at the inner and outer land is determined empirically and is represented by Equation (8). Z is an empirical constant determined using finite element methods.

$$houter = Z \times hinner \qquad (8)$$

Simultaneous solution of Equations (6), (7b), and (8) yields the hydropad pressure, *Pt*, and the gaps at the inner and outer lands, *hinner* and *houter* respectively. These values are then used to calculate the leakage based on the viscosity of the process fluid.

The orifice feed slot sizing sets the pressure in the hydropad. The pressure profile of the seal face and therefore the operating gap of the seal is determined by the hydropad pressure. As a result, there is a direct correlation between the feed slot sizing and the leakage across the hydrostatic throttle bushing, as shown in Figure 12. The effects of varying the orifice feed slot size can be analyzed with all other variables held constant.

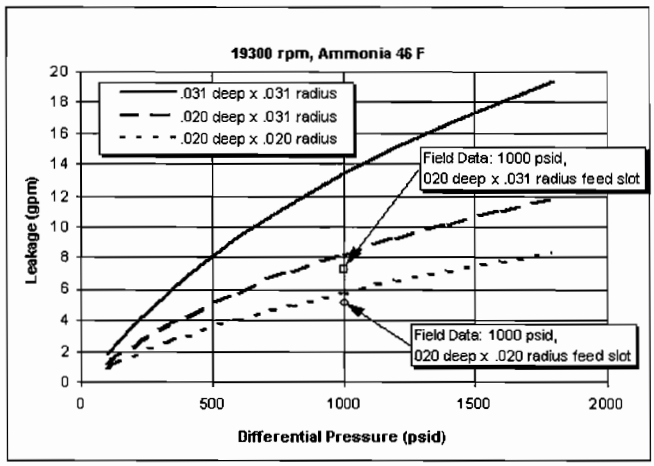

Figure 12. Feed Slot Orifice Size Effects on Leakage Rates.

Because of the ability to input differing geometry, fluid properties, and machine characteristics, the model allows for a parametric study of varying process and build conditions. Figures 13 and 14 show the effects on performance of speed and temperature (viscosity), respectively. Field data points are from field installation discussed in the FIELD TEST PROGRAM section below.

The model proved to be a valuable tool providing high correlation between predicted leakage values and actual leakage values. Correlation of data from field installations, as discussed below, is shown in Figures 12 and 13.

WATER TESTING

Initial testing of the hydrostatic throttle bushing was carried out on water. The test loop, shown in Figure 15, included two high speed, single stage centrifugal pumps; one modified to accept the hydrostatic throttle bushing and the second to generate pressure in the test loop. Also installed in the loop was a buffer tank for process supply and a magnetic flowmeter to monitor leakage flow. Two pressure gauges, one upstream and one downstream of the throttle bushing, monitored pressure drop across the face. Finally, a heat exchanger kept the circulating fluid at a constant temperature.

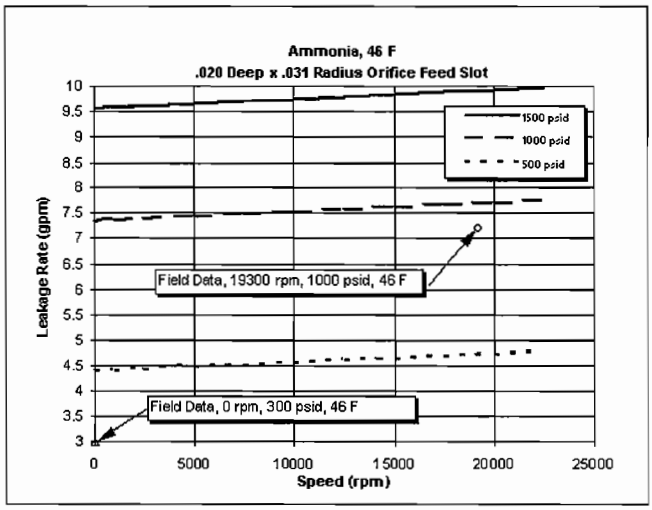

Figure 13. Speed Effects on Performance.

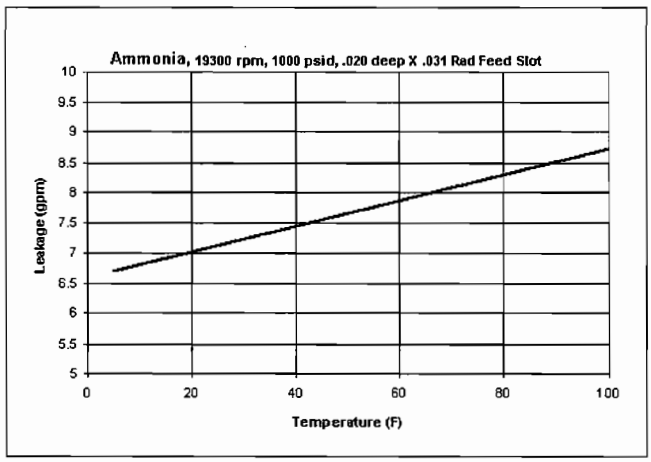

Figure 14. Temperature (Viscosity) Effects on Performance.

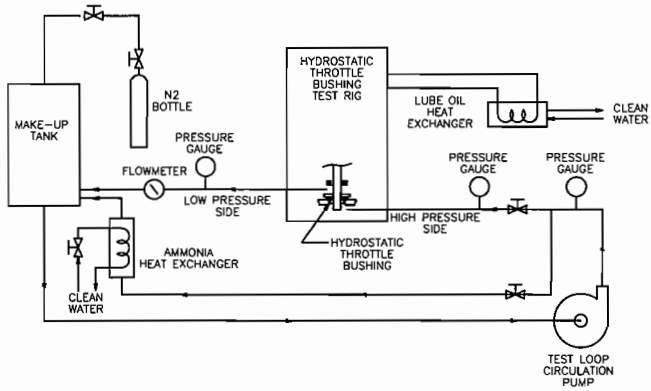

Figure 15. Water/Ammonia Test Rig, Hydrostatic Throttle Bushing.

All testing was carried out with an Ultimet® hydrostatic throttle bushing and a solid tungsten carbide mating ring. Goals of the tests were to determine:

- Leakage flow as a function of pressure and speed.
- "Life" verification of the throttle bushing.
- Cavitation resistance of the modified geometry.
- The effects of running dry.
- The effect of numerous starts and stops.

Start/stop tests were conducted in both a dry and a wetted state. The use of a variable speed drive on the motor allowed testing at several speeds: 7000 rpm, 14,000 rpm, and 21,000 rpm. Over 200 hours of continuous operation were achieved with positive results. Data points taken at the three test speeds were matched by the mathematical model. It was found that speed affects on the throttle bushing leakage were minimal, with only a 20 percent increase in leakage between 7000 rpm and 21,000 rpm at the same pressure drop, as shown in Figure 16. Overall, leakage rates were well within acceptable limits at the tested pressure drop.

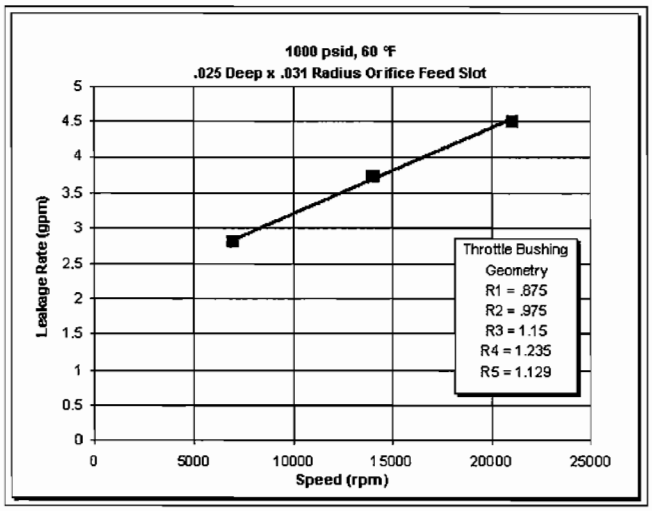

Figure 16. Water Test Data.

Testing showed that the hydrostatic throttle bushing lifted off the mating ring in a static condition when pressures reached approximately 200 psi. Because of this, the throttle bushing was never in a contacting condition during standard testing, and no wear occurred. Metcalfe's (1972) design factor regarding a minimum pressure drop to prevent contact was confirmed from this aspect of the testing. As long as contact is prevented, the throttle bushing should achieve infinite life.

Additional support for infinite life was found with a visual inspection for signs of cavitation damage. After over 200 hours of operation, there were no visible signs of cavitation damage to any part of the throttle bushing. This was a positive sign since previous operation of a "typical" style hydrostatic seal had shown significant damage over a shorter period of operation.

Start/stop testing showed similarly positive results as long as a pressure differential of at least 200 psi was maintained across the throttle bushing. Once the pressure differential was reduced however, contact occurred. One deficiency cited in the literature about slot fed hydrostatic seals concerns wear that may occur on contact. Metcalfe (1972) indicates wearing can result in reduction in area of the feed slot (orifice) size. Once the size is reduced, the pressure in the hydropad is reduced, exacerbating the wear through higher force contact. In this case, because the hydrostatic throttle bushing was constructed of a hard material, the wear during contact was minimized significantly. After 20 starts and stops at only 12 psi differential, there was scuffing of both faces; however the material removal was small, so the effect on the feed slots was minimal. Even with the cobalt based material mentioned previously, however, continuous operation in a contacting condition for extended duration did cause damage that would adversely affect the performance of the throttle bushing. As a result, contact must be minimized by ensuring sufficient pressure drop across the face for lift off prior to startup.

AMMONIA TESTING

The next phase of validation testing was on liquid ammonia. Ammonia is an ideal candidate for hydrostatic seal technology. As with light hydrocarbons, it has low viscosity, evaporates easily, and has poor lubricating properties. Testing on ammonia was carried out utilizing the seal test rig constructed for the water tests, except a triplex plunger pump replaced the centrifugal circulation pump. Data obtained at a single point were used to further validate the mathematical model. At a pressure drop of 300 psig, the leakage rate was 5.5 gpm.

FIELD TEST PROGRAM

The final phase of validation was field testing in a centrifugal pump. Again, the high speed, high pressure, two stage pump was the test vehicle. A proposal was presented to a nitrogen operations plant in Carseland, Alberta, Canada. This facility has two pumps installed in the ammonia stream of their urea production facility. These pumps had been in operation since 1976, utilizing a series of four dynamic rotors and stators to achieve the pressure drop necessary to protect the mechanical process seal. Process conditions are shown in Table 2.

Table 2. Centrifugal Pump Process Conditions.

Process	Urea, ammonia stream
Flow	437 US gpm
Head	8143 ft
Specific gravity	0.60
Power	1067 bhp
Speed	19,278 rpm
Suction pressure	319 psig

The configuration of these pumps was API Plan 32 (API 610, Eighth Edition) with single seals on stage one and stage two, each with a filtered ammonia flush. The seal flush on stage one and stage two was introduced into the respective stuffing boxes to keep the mechanical seals clean and cool. Figure 17 represents the specific process diagram for this installation. Whereas stage one flush entered the process stream directly, stage two was routed through the dynamic rotors prior to entering the process stream. Assembly experiences encountered with the dynamic rotor system proved difficult. Clearances on the dynamic rotors are close, and proper assembly is imperative, thus some hard learned assembly technique experience was gained during the first couple of years after pump installation. Despite initial difficulties, the pumps have operated reliably since 1976. The site was willing, despite being comfortable with the dynamic rotor configuration, to install the throttle bushing in their ammonia pump due to its simplicity.

The hydrostatic throttle bushing was installed in September 1997. The stage one seal flush configuration was unchanged. The stage two flush system was rerouted to accommodate the leakage flow from the hydrostatic throttle bushing. Flush fluid for stage two came from the process stream behind the impeller. The flush flowed across the throttle bushing to drop the pressure, prior to entering the stuffing box. After flushing the mechanical seal, the flush fluid was removed externally where it had previously been introduced, as shown in Figure 18. Leakage flowrate was monitored by an inline flowmeter after exiting the pump. The flow was routed to the ammonia storage tank that was at atmospheric pressure. In order to prevent vaporization of the ammonia in the stuffing box, a back pressure regulator was utilized. Stuffing box pressure was maintained at 100 psig greater than suction pressure to the pump. A pressure gauge monitored the stuffing box pressure

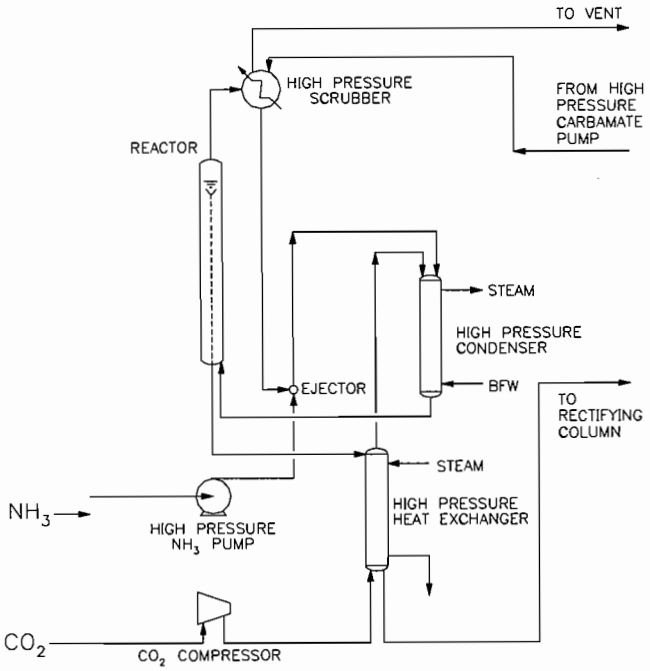

Figure 17. Process Diagram, Carseland Facility.

and a pressure switch was installed to protect the mechanical face seal in the event of throttle bushing failure.

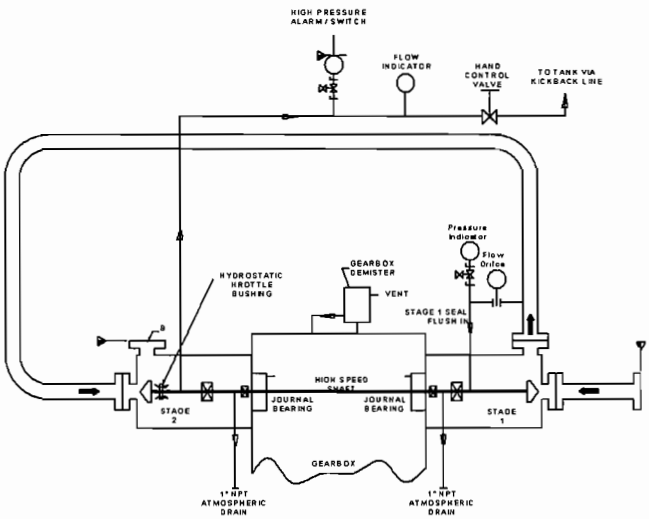

Figure 18. Process Diagram of Carseland Facility After Installation of Hydrostatic Throttle Bushing.

Prior to startup of the unit on the ammonia process, static leakage readings were taken with full suction pressure to the pump. The throttle bushing flow was approximately 3 gpm at a pressure drop of 300 psig. The unit was then started and leakage increased to 10 gpm at a pressure drop of 1000 psig. These values correlate well to the expected pressure drop and flow, based on analysis with the model, as shown in Figure 13. During commissioning, a number of process upsets resulted in repeated pump starts with no adverse effect on the hydrostatic throttle bushing. Shortly after startup of the unit, numerous problems encountered with the back pressure regulator prompted its removal. In its place, a throttle valve was installed that could be adjusted manually to set the stuffing box pressure in the pump. It was felt that fluctuations in process conditions would be within an acceptable range to utilize a fixed orifice to maintain a minimum pressure in the stuffing box. By using an adjustable hand valve, the fixed orifice simply became an adjustable orifice, which provided more flexibility. Site operators showed a strong preference for this configuration.

In March 1998, the plant was shut down, which provided the opportunity to inspect the hardware that had been running for six months. Visual inspection of the hydrostatic throttle bushing showed why the conditions had not changed. There were no signs of cavitation in the feed slots, the orifice pockets, or on the inner and outer lands, as can be seen in Figure 19. A small amount of erosion appeared on the leading edge, outer corner of each recess. The area was so small it was difficult to discern the exact phenomena occurring in these locations. Although there was slight circumferential grooving indicating light contact with the mating ring, the effects on the face were slight and of little concern. Considering the severe conditions the throttle bushing had endured during the multiple startups, it had performed above expectations. After visual inspection was complete, the throttle bushing was reinstalled in the pump.

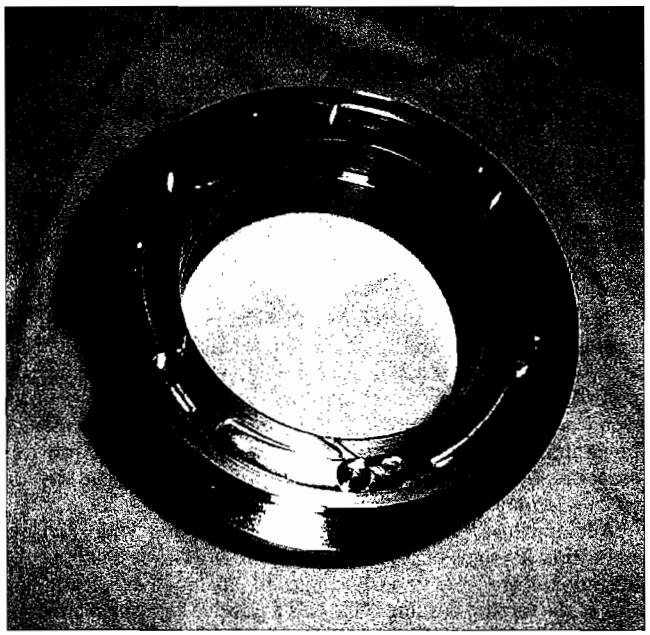

Figure 19. Hydrostatic Throttle Bushing After Six Months Continuous Operation.

As with the throttle bushing, there were circumferential marks on the mating ring indicating contact, although the effects were minor. There was a residue on the surface corresponding to the throttle bushing face, and there was a region corresponding to the outer perimeter of the throttle bushing that showed either heavier buildup of residue or erosion. Subsequent inspection revealed that the mating ring had experienced some cavitation damage at the outer perimeter, outside the face of the hydrostatic throttle bushing. The region of contact with the throttle bushing was not affected and it is expected that the cavitation damage will not progress further. Because of the success of the throttle bushing on the first unit, the standby unit was converted to the throttle bushing hardware in June 1998. The field test site has expressed much satisfaction with the performance of the hydrostatic throttle bushing.

COMMERCIAL APPLICATION

The first commercial application of the hydrostatic throttle bushing was in a two stage, ammonia feedpump, similar to the field test pump, located in Redwater, Alberta, Canada. The urea process

diagram is shown in Figure 20. The unit had been purchased as an upgrade for an earlier model that had been operating since 1984. The motivation for replacement was due to production increases that demanded additional horsepower. The pump is different from the pump noted previously, in that the extra head requires extra speed. It was decided to upgrade the pump with an improved model that incorporated the latest design features, including the hydrostatic bushing. Although the upgrade was necessary, based on increased product demand, the pump and spare had provided 100 percent availability for process during the 14 year period of operation. The biggest difficulty over the operating life had been with the mechanical face seals. The maximum seal life had only been 24 months. Special material selection and the need for extremely tight machining tolerances on the multicomponent stackup meant high purchase and refurbishing costs. The original pump utilized tandem seals on both stages with a water buffer supplied between the inboard and outboard seals: 250 psig to the first stage and 600 psig to the second stage. The inboard seal of the first stage used an API Plan 13 (API 610, Eighth Edition) flush, whereas the second stage had a filtered API Plan 11 (API 610, Eighth Edition) flush from the pump discharge. The second stage used a single dynamic rotor for reduction of the stuffing box pressure. The new seal design abandons the tandem arrangement in favor of a dual seal design with water as the buffer. The dynamic seal rotor assembly is replaced by the hydrostatic throttle bushing. Process conditions for the original and upgraded pumps are shown in Table 3.

Table 3. Process Conditions for the Original and Upgraded Pumps.

	Original	Upgrade
Flow	403 US gpm	602 US gpm
Head	11,849 ft	12,090 ft
Specific gravity	0.58	0.60
Power	1450 bhp	1943 bhp
Speed	22,100 rpm	21,083 rpm
Suction pressure	300 psig	300 psig
Discharge pressure	3275 psig	3444 psig

The unit was performance tested on water in the manufacturer's shop. Performance of the hydrostatic throttle bushing was monitored during testing. For this application, the throttle bushing was designed to drop the pressure by 1400 psid at a leakage flowrate of 7 gpm to 8 gpm. Initial testing showed results that did not conform to the results as previously seen with predictions from the mathematical model. The leakage at 1400 psig was much lower than expected at 1.5 gpm. Investigation uncovered the fact that a reverse rotation throttle bushing had actually been installed in the unit. It was determined that significant entrance losses due to the fluid circumferential velocity at the entrance to the feed slots were reducing the pressure leading into the hydropad. The reduced hydropad pressure caused the throttle bushing to operate at a reduced gap, thereby affecting the leakage across the face. Further testing showed that simply increasing the feed slot size increased the hydropad pressure and thus the operating gap of the seal, which thereby returned the leakage to predicted levels. The unit was fitted with the correct throttle bushing prior to shipment; however, the testing had proven that it could operate under reverse rotation conditions.

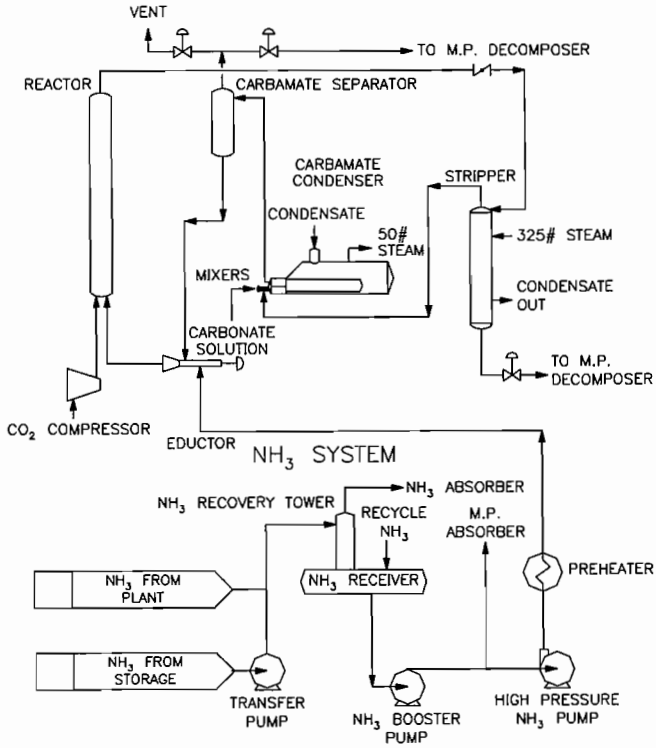

Figure 20. Process Diagram, Redwater Facility.

In July 1998, the unit was commissioned. The pump has been operating successfully since, with leakage rates across the hydrostatic throttle bushing being very close to the predicted levels of 7.5 gpm at 1500 psid. As with the Carseland field test site, the Redwater site has expressed a high level of satisfaction with the operation of the hydrostatic throttle bushing in this application.

CONCLUSION

The hydrostatic throttle bushing has proven to be a reliable yet simple alternative to the dynamic rotor system it replaced. Field operation shows that the cavitation damage experienced on earlier hydrostatic seals has been eliminated through the use of cavitation resistant materials and unique modifications to the face geometry. Rigorous field operation, including multiple upsets and subsequent startups and shutdowns, has proven the robustness of the hydrostatic throttle bushing design. As long as there is a minimum pressure drop across the throttle bushing, it has proven to operate continuously in a noncontacting state. Even when contact has occurred, the effect has been minimal. Dry run testing has shown that even with heavy wear, to the extent that the hydrostatic features are minimized, the results are not catastrophic. Testing has shown that failure of the hydrostatic throttle bushing results only in an increase or decrease of leakage. Monitoring leakage flow provides a simple means of monitoring the condition of the hydrostatic throttle bushing. Successful field operation on ammonia provides strong support for future application in light hydrocarbons. Virtually any application involving a relatively clean process, where there is a high pressure drop required to protect the mechanical face seal, is a viable candidate for this technology.

NOMENCLATURE

(Reference Figure 11)

R1	=	Inner radius of hydrostatic throttle bushing face (in)
R2	=	Inner radius of hydropad (in)
R3	=	Outer radius of hydropad (in)

R4	=	Outer radius of hydrostatic throttle bushing face (in)
R5	=	Balance diameter of hydrostatic throttle bushing (in)
b	=	Feed slot orifice width (in)
t	=	Feed slot orifice depth (in)
Rgrv	=	Feed slot orifice radius (in)
Pe	=	Mechanical stuffing box pressure (psi)
Ps	=	Sealed pressure (psi)
Pt	=	Hydropad pressure (psi)
Cd	=	Feed slot orifice coefficient
μ	=	Fluid viscosity (lb-sec/in^2)
ρ	=	Fluid density (lb/in^3)
ω	=	Rotational speed (rad/sec)
Fclose	=	Closing force, due to sealed pressure (lbf)
Fspring	=	Spring force (lbf)
Fthrust	=	Thrust load on seal face (lbf)
Fhydrodynamic	=	Thrust due to hydrodynamic effects (lbf)
Yin	=	Empirically derived constant
Yout	=	Empirically derived constant
Z	=	Empirically derived constant
Hinner	=	Gap at inner land (in)
Houter	=	Gap at outer land (in)

REFERENCES

API Standard 610, 1995, "Centrifugal Pumps for Petroleum, Heavy Duty Chemical, and Gas Industry Services," Eighth Edition, American Petroleum Institute, Washington, D.C.

Cheng, H. S., Chow, C. Y., and Wilcock, D. F., 1968, "Behavior of Hydrostatic and Hydrodynamic Noncontacting Face Seals," Journal of Lubrication Technology, pp. 510-519.

Haynes International, Inc., 1994, "Ultimet® Alloy," Kokomo, Idaho, Bulletin No. H-2082B.

Laurenson, I. T. and O'Donoghue, 1978, "Hydrostatic Seal Design," Journal Mechanical Engineering Science, IMechE, *20*, (3), pp. 159-167.

Laurenson, I. T., O'Donoghue, and Hooke, C. J., 1973, "A Slot Fed Multirecess Hydrostatic Seal," Sixth International Conference on Fluid Sealing, Munich, German Federal Republic, pp. G2-15 - G2-23.

Lebeck, A. O., 1991, *Principles and Design of Mechanical Face Seals,* New York, New York: John Wiley and Sons, Inc.

Mallaire, F. R., Nelson, L. H., and Buckmann, P. S., 1969, "Evaluation of Wear Ring Seals for High-Speed, High-Pressure Turbopumps," Transactions of the ASME, pp. 438-450.

Metcalfe, R., 1972, "An Analysis and Optimization of Geometry for Pocket and Orifice-Type Hydrostatic Face Seals," Atomic Energy of Canada Limited, AECL-4145.

Prouty, W. C. and Bond, J. C., 1998, "Hydrostatic Seal," U.S. Patent No. 5,755,817.

ACKNOWLEDGEMENTS

The authors wish to thank Sundstrand Fluid Handling Corporation and Agrium for their support of this work. Special thanks go to John Bond, John Sidelko, and Fronz Robinson of Sundstrand; Bernie Daniels, Roger Atkinson, and Larry Matheson of Agrium Carseland Nitrogen Operations; and Gerry Kydd, Peter Bizuk, and Elmer Breit of Agrium Redwater Nitrogen Operations.